Research paper

In vitro cytotoxicity and DNA interaction study of phosphanegold(I) complexes with dithiocarbamate ligands

Said S. Al-Jaroudi, Muhammad Altaf, Adam A. Seliman, Shipra Yadav, Farukh Arjmand, Ali Alhoshani, H.M. Korashy, Saeed Ahmad, Anvarhusein A. Isab

PII: S0020-1693(17)30336-5
DOI: http://dx.doi.org/10.1016/j.ica.2017.04.040
Reference: ICA 17545

To appear in: *Inorganica Chimica Acta*

Received Date: 5 March 2017
Revised Date: 17 April 2017
Accepted Date: 19 April 2017

Please cite this article as: S.S. Al-Jaroudi, M. Altaf, A.A. Seliman, S. Yadav, F. Arjmand, A. Alhoshani, H.M. Korashy, S. Ahmad, A.A. Isab, *In vitro* cytotoxicity and DNA interaction study of phosphanegold(I) complexes with dithiocarbamate ligands, *Inorganica Chimica Acta* (2017), doi: http://dx.doi.org/10.1016/j.ica.2017.04.040

In vitro cytotoxicity and DNA interaction study of phosphanegold(I) complexes with dithiocarbamate ligands

Said S. Al-Jaroudi[a], Muhammad Altaf[b], Adam A. Seliman[a], Shipra Yadav[c], Farukh Arjmand[c], Ali Alhoshani[d], H. M. Korashy[d] Saeed Ahmad[e], and Anvarhusein A. Isab[a]*

[a] *Department of Chemistry, King Fahd University of Petroleum and Minerals, Dhahran 31261, Saudi Arabia.*
[b] *Center of Research Excellence in Nanotechnology, King Fahd University of Petroleum & Minerals, 31261 Dhahran 31261, Saudi Arabia.*
[c] *Department of Chemistry, Aligarh Muslim University, Aligarh 202002, Uttar Pradesh, India.*
[d] *Pharmacology and toxicology department College of pharmacy King Saud University Riyadh 11451, Saudi Arabia.*
[e] *Department of Chemistry, College of Sciences and Humanities, Prince Sattam bin Abdulaziz University, Al-Kharj 11942, Saudi Arabia*

Abstract

A new series of phosphanegold(I) dithiocarbamate complexes with general formula $[Au(PR_3)(S_2CNR'_2)]$ **1-5** (Where R= Methyl, ethyl, isopropyl and R'= Methyl, ethyl) were synthesized and characterized by elemental analysis, FTIR and multinuclear NMR spectroscopy. The molecular structure of complex **1** was determined by single crystal X–ray crystallography, which revealed linear geometry around the Au(I) metal center. The *in vitro* cytotoxicity of all Au(I) complexes was studied against two A549 and HepG2 human cancer cell lines. All the complexes showed significantly higher potency (4 to 6-fold for A549 and 3 to 5-fold for HepG2 cell line than commercial chemotherapeutic drug cisplatin. The *in vitro* DNA binding abilities of Au(I) complexes **1-5** were examined by employing different biophysical techniques, *viz.*, UV–Vis titrations, fluorescence spectroscopy and circular dichroism. The UV–Vis titration of Au(I) complexes with CT DNA revealed that complexes bind to CT DNA *via* electrostatic interactions, and the intrinsic binding constant (K_b) values for **1-5** were found to be 3.90×10^4, 4.74×10^4, 6.81×10^4, 8.53×10^4 and 2.48×10^4 M^{-1} respectively. Which suggested a higher binding propensity for complex **4**. In addition, molecular docking studies of the Au(I) complexes were performed with B–

DNA to visualize the preferential docking position, and the results revealed that the complexes bind to the adenine–thymine residues in the minor groove of the DNA.

Keywords: Dithiocarbamate Phosphine Au(I**)** complexes, Anticancer, A549 lung cancer cell line and HepG2 cancer cell line, CT-DNA binding studies, mononucleotide interaction and molecular docking

---

Author for correspondence: Dr. A. A. Isab; aisab@kfupm.edu.sa

1. Introduction

The development of new metallo-therapeutic drugs with different pharmacological activity from platinum drugs is one of the major goals of modern bioinorganic and bio-organometallic medicinal chemistry research [1-7]. Gold complexes have recently gained considerable attention as a class of compounds whose pharmacodynamic and kinetic properties differ from those of cisplatin and that have strong cell growth-inhibiting effects [2, 3]. The field of medicinal inorganic chemistry has gained prominence through the serendipitous discovery of the cytotoxic properties of cisplatin by Rosenberg [8]. Despite the great success of cisplatin and its analogues, the administration of platinum drugs manifests systemic toxicity and clinical inefficiency against resistant tumors, which limit their domain of applicability [9]. Therefore, considerable efforts are being made to circumvent the side effects, to enhance the cytotoxicity profile and to augment the efficacy and specificity of the prevalent antitumor drugs [10-11]. Among the emerging class of non-platinum antitumor agents, gold(I) complexes have recently gained attention because of their strong toxicity toward malignant cells, which is generally accompanied by non-cisplatin-like pharmacodynamics, pharmacokinetic properties and mechanisms of action [12-13]. The incorporation of a gold metal center into drug scaffolds offers vast potential for creating promising metal-based drug candidates with significant cytostatic and/or cytotoxic effects against various cancer cell lines [14-15]. The antirheumatic drug auranofin and a number of its analogues have shown significant in vitro and in vivo cytotoxic activity. Among them, phosphine gold(I) complexes proved to be the most potent. Literature reports reveal that phosphine ligand in gold(I) increases the potency and/or generates selectivity for various biological targets. The antitumor activity is modulated by the presence of phosphine substituents in phosphine gold(I) complexes, in addition to the nature of other auxiliary ligands present. Dithiocarbamate units tethered to gold(I) phosphine motifs offer the potential ability to prevent interactions of the metal center with sulfur-containing proteins, thereby reducing renal toxicity [16-17]. Dithiocarbamates are bidentate S,S′-chelating ligands that possess an extraordinary ability to

form stable coordination complexes with metal ions due to the "chelation effect." The complex **4** ([Au(I)(Et_3P)(S_2CNEt_2)]) was previously reported showing significant antiproliferative effects against several human cancer cell lines and a potent antibacterial activity [18-20]. Also, the synthesis and characterization of complex **2** ([Au(I)(Et_3P)(S_2CNMe_2)]) were reported in the literature using ^{31}P NMR to mimic ligation site of "Et_3P─Au" moiety to the protein such as albumin [21].

There is a paucity of literature regarding the interaction of Au(I) complexes with DNA [22], a primary target that plays a central role in the onset of apoptosis, which makes DNA interaction studies necessary to ascertain the chemotherapeutic potential of metal complexes. Metal complexes are known to damage the replication process of DNA by either covalent or noncovalent interactions. In covalent binding, the labile ligand of the complexes is replaced by a nitrogenous base of DNA, such as N7 of guanine. In contrast, noncovalent interactions include intercalation, which involves the partial insertion of aromatic heterocyclic rings of ligands between the DNA base pairs, and electrostatic and groove (surface) binding, which involves the binding of metal complexes along the outside of the DNA helix [23-24]. Following our previous studies on mixed phosphine gold(I) dithiocarbamate compounds with antitumor activity [25-26] and in continuation of our intrinsic interest in the synthesis of gold(I) complexes to better understand the chemical and physical behavior of biologically relevant dithiocarmato(phosphine)gold(I) complexes, gold(I) complexes 1-**5** have been synthesized and fully characterized by elemental analysis, FTIR, NMR measurements and UV-Vis spectroscopic techniques. Scheme 1 shows the structures of the reported complexes. Their cytotoxicity has been tested in vitro against the lung cancer cell lines A549 and liver hepatocellular cancer cell lines HepG2. The presence of a linear S-Au-PR_3 moiety that could act selectively in cancer tissues and undergo biological ligand exchange reactions, thereby exhibiting potent cytotoxic activity. In the current study, interaction studies of Au(I) synthesized complexes 1-**5** were conducted with CT-DNA by employing different biophysical spectroscopic methods. The

title complexes showed significant cytotoxic effects and were found to be more active than cisplatin.

2. Experimental

2.1. Chemicals, Cell lines and Cell cultures

Ethidium bromide (EB), sodium N,N-dimethyldithiocarbamate monohydrate (DMDC) or sodium N,N-diethyldithiocarbamate trihydrate (DEDC) were purchased from Sigma-Aldrich. Tris(hydroxymethyl)aminomethane (tris–buffer) (Merck), adenosine–5'–monophosphate disodium salt (5'–AMP), cytidine–5'–monophosphate disodium salt hydrate (5'–CMP), guanosine–5'–monophosphate disodium salt (5'–GMP) thymine–5'–monophosphate (5'–TMP) and CH_3OH were obtained from Fluka Chemicals Co. and were stored at –20 °C. Disodium salt of ct–DNA purchased from Sigma Chem. Co. and was stored at 4 °C. All reagents as well as solvents were used as received. Human lung cancer cell lines A549 and liver hepatocellular cancer cell lines HepG2 were provided by American Type Culture Collection. MTT (3-(4,5-Dimethylthiazol-2-yl)-2,5-diphenyltetrazolium bromide, a yellow tetrazole) was purchased from Sigma Chemical Co, St. Louis, MO, USA.

2.2. Synthesis of $[Au(PR_3)(S_2CNR'_2)]$ (1-5) complexes.

Gold(I) complexes (**1-5**) were synthesized according to a reported procedure [27]. To a suspension of chloro(trialkylphosphine)gold(I) (0.5 mmol) in methanol (20 mL), cooled at 0 ^oC in ice bath under inert conditions using nitrogen gas flow, was added dropwise sodium dimethyldithiocarbamate (DMDC) or sodium diethyldithiocarbamate (DEDC) (0.5 mmol) solution in 5 mL of methanol with continuous stirring for 2h. The clear yellow or orange solution obtained was filtered to remove insoluble materials. The slow evaporation of solution at RT afforded a yellow or orange solid. The final solid product was washed with distilled water (3 x 10 mL) to

remove NaCl salt and gold(I) complexes **1-5** were collected as a yellow or orange solid. The yield of the complexes **1-5** was in the range of 81-86%. Elemental analysis data of gold(I)complexes **1-5** is tabulated in Table 1S.

2.3. Electronic Spectra

Electronic spectra were obtained for the gold(I) complexes using Lambda 200, Perkin-Elmer UV-Vis spectrometer. UV-Vis spectroscopy was used to determine the stability of the complexes in DMSO. Electronic spectra were recorded on freshly prepared of each complex in buffer solution (pH =7) at room temperature.

2.4. Mid and Far-IR studies

IR spectra of the dithiocarmate ligands and their phosphanegold(I) complexes **1-5** were recorded on a Perkin-Elmer FTIR 180 spectrophotometer using KBr pellets over the range 4000-400 cm^{-1}. Whereas, Far-infrared (FIR) spectra were recorded at 4 cm^{-1} resolution at room temperature using CsCl disks on a Nicolet 6700 FT-IR with Far-IR beam splitter.

2.5. Solution NMR measurements

The ^{1}H (500.01 MHz), ^{13}C (125.6 MHz), and ^{31}P (202.35 MHz) NMR spectra were recorded on a Jeol JNM-LA 500 NMR spectrophotometer at 297 K. The ^{1}H and ^{13}C chemical shifts were referenced relative to TMS. The spectral conditions were: 32 k data points, 0.967 s acquisition time, 1.00 s pulse delay and 45 pulse angle. ^{31}P NMR spectra were measured using 0.269 s acquisition time, 20.00 s pulse delay and 6.20 μs pulse with ^{1}H broadband decoupling. ^{31}P NMR chemical shifts were measured relative to the internal reference 85% H_3PO_4 (0.0 ppm) according to scheme 1.

2.6. Solid state NMR studies

^{13}C solid-state NMR spectra were performed on a Bruker 400 MHz spectrometer at ambient temperature of 25^{o}C. Samples were packed into 4 mm zirconium oxide rotors. Cross polarization and high power decoupling were employed. Pulse delay of 7.0 s and a contact time of 5.0 ms were used in the CPMAS experiments. The magic angle spinning rates were 4 and 8 kHz. Carbon chemical shifts were referenced to TMS by setting the high frequency isotropic peak of solid adamantane to 38.56 ppm.

2.7. X-ray diffraction analysis

Suitable crystals of complex **1** was obtained as yellow block by recrystallization of final product from mixture of dichloromethane and ethanol (1:1) solution. X-ray diffraction data was collected at 173 K on a Stoe Mark II-IPD System [28] equipped with a two-circle goniometer and using MoKα graphite monochromatic radiation. Diffraction data for **1** was collected using ω rotation scans of 0°–180° at ϕ = 0° and of 0°–180° at ϕ = 90° with step Δω = 1.0°, exposures of 1 minute per image, 2θ range = 2.29°–59.53° and d_{min}–d_{max} = 17.779–0.716 Å. The distance between the imaging plate and the sample was 100 mm whereas structure was solved by direct methods using the program SHELXS-97 [29]. The refinement and all further calculations were carried out using SHELXL-97 [29]. The H-atoms were either located from Fourier difference maps and freely refined or included in calculated positions and treated as riding atoms using SHELXL default parameters. The non-H atoms were refined anisotropically, using weighted full-matrix least-squares on F^2. Semi-empirical method were applied using MULSCANABS routines in PLATON [30]. A summary of crystal data and refinement details for complex **1** is given in Table 1. The structure of complex **1** was drawn using PLATON [31].

2.8. Computational Study

The structure of complex (1), [Au(PMe_3)(S_2CNMe_2)] was optimized without any geometrical constrains using GAUSSIAN09 program [32]. The hybrid B3LYP density functional (the three-parameter Becke functional with correlation from the Lee-Yang-Parr functional) [33-34] with the Los Alamos National Laboratory-2 double-ζ (LANL2DZ) basis set [35-37] was employed in this study. The calculated data were consistent with our experimental finding. Moreover, stationary points have been confirmed by frequency calculation.

2.9. Cell cultures

Human lung cancer cell lines A549 and liver hepatocellular cancer cell lines HepG2 were grown in Dulbecco's modified Eagle's medium (DMEM) supplemented with 10% Fetal Bovine Serum (FBS), and 1% penicillin (10,000 units), streptomycin (10 mg), in 74 cm^2 flask and incubated until 80% confluences obtained in humidified environment of, 5% CO_2, 95% air, 37 ^oC.

2.10. MTT assays for anticancer activity of gold(I) complexes (1-5)

A series of concentrations of gold(I) complexes (**1–5**) and cisplatin were prepared in DMEM. Cancer cells were seeded and maintained in quadruplicate in a 96-well tissue culture plate at 5 X 10^4 cells per well in 200 µL of same medium. The cancer cells were incubated 24 hours before the treatment. All complexes were dissolved in 50% DMSO. Therefore, DMSO was used as a negative control. The final DMSO concentration, in each well, was less than 0.1%.

The cancer cells were treated with the synthesized complexes **1-5** along with the cisplatin and the resultant cultures were incubated for 24 h. The medium of wells was discarded and 100 µL DMEM containing MTT (3-(4,5-dimethylthiazol-2-yl)-2,5-diphenyltetrazolium bromide) (5 mg/mL) was added to the wells and incubated in a CO_2 incubator at 37 ^oC in the dark for 4 h. After incubation, a purple colored formazan (artificial chromogenic dye, a product of the reduction of water insoluble tetrazolium salts e.g., MMT by dehydrogenases and reductases) in the cells is produced and

appeared as dark crystals in the bottom of the wells. The medium of culture was discarded from each well carefully to avoid disruption of the monolayer. 100 µL of isopropanol was added in each well. The solution was thoroughly mixed in the wells to dissolve the formazan crystals which ultimately results into a purple solution. The absorbance of the 96-well plate was taken at 570 nm with Mithras^{2}LB943 against reagent blank. All data presented are mean± standard deviation.

2.11. DNA binding

DNA binding experiments which include absorption spectral titrations, fluorescence and circular dichroism conformed by the standard methods and practices previously adopted in our laboratory [38-40].

2.11.1 Absorption spectral experiments

Absorption spectral titration experiments were performed at constant concentration of the complexes with varying CT–DNA concentration. The absorbance (A) of the most shifted band of investigated complexes was recorded after successive addition of CT–DNA. A reference cell contained DNA alone to nullify the absorbance due to the DNA at the measured wavelength. From the absorption titration data, the intrinsic binding constant (K_b) of the complexes with CT–DNA were determined using Wolfe–Shimmer equation [41].

$$\frac{[DNA]}{\varepsilon_a - \varepsilon_f} = \frac{[DNA]}{\varepsilon_b - \varepsilon_f} + \frac{1}{K_b(\varepsilon_a - \varepsilon_f)} \quad (1)$$

Where ε_a, ε_f and ε_b correspond to A_{obsd}/[Complex], the extinction coefficient for free complex, and the extinction coefficient for the complexes in the fully bound form respectively. Plot of [DNA]/ε_a–ε_f vs. [DNA], where [DNA] is the concentration of DNA in the base pairs, gives K_b as the ratio of slope to the intercept.

2.11.2. Fluorescence spectral studies

Fluorescence experiments were carried out at constant concentration of the complexes with increasing CT–DNA concentration. The binding constant *K* of the metal complexes was determined from Scatchard Eqs. (2) and (3) by employing emission titration [42-43]

$$C_F = C_T (I/I_o – P) (1 – P) \quad (2)$$

$$r/C_F = K (n – r) \quad (3)$$

where, C_F is the free probe concentration, C_T is the total concentration of the probe added, I and I_o are fluorescence intensities in presence and absence of CT–DNA, respectively and P is the ratio of the observed fluorescence quantum yield of the bound probe to that of the free probe. The value P was obtained as the intercept by extrapolating from a plot of I/I_o vs. 1/[DNA], r denotes ratio of C_B ($C_B = C_T – C_F$) to the DNA concentration, i.e., the bound probe concentration to the DNA concentration, *K* is the binding constant and C_F, is the free metal complex concentration and ‘‘n’’ is the binding site number.

Luminescence titrations involving quenching experiments were conducted by adding increasing concentration of complexes to a fixed concentration of EB–DNA system. Tris–HCl buffer was used as a blank to make preliminary adjustments. Stern–Volmer quenching constant, K_{sv} was obtained from the following equation [44]

$$I_0/I = 1 + K_{SV}.r \quad (4)$$

Where r is the ratio of total concentration of complex to that of DNA and I_o and I are the fluorescence intensities of EB in the absence and presence of complex.

3. Results and Discussion

3.1. Electronic spectra

The λ_{max} values obtained from UV-Vis spectral studies of complexes are shown in Table 2S. The optical electronic absorption spectra in solution generally show a similar pattern for all the complexes. The gold(I) complexes (**1-5)** are characterized by two intense absorptions in the range

270-272 and 321-333 nm, which were attributed to the intramolecular intraligand transition corresponding to $\pi \rightarrow \pi^*$ in the NCS and CSS moieties, respectively [45-47]. These results indicate the presence of partial double bond character in N-C group, which supports the monodentate complexation of the dithiocarbamate ligands.

3.2. Mid and Far-IR spectroscopic studies

The most significant bands recorded in the FTIR spectra of the dialkyldithiocarbamate ligands and gold(I) complexes **1-5** are reported in Tables 3S and 4S. The interpretation of the FTIR spectra of dithiocarbamate complexes of transition metals has aroused considerable interest both in finding the mode of coordination and evaluating the nature of bonding in these complexes. In examining the infrared spectra of dithiocarbamate complexes, the three main areas of interest are three regions 1580-1450, 1060-940 and 430-250 cm^{-1} due to ν(C−N) stretching vibrations, ν(C−S) and ν(M−S) respectively [48].

Gold(I) phosphane complexes **1-5** containing dialkyldithiocarbamate ligands exhibit a characteristic band in the range (1476–1507) cm^{-1} that is assignable to the N–CSS stretching mode [49-50]. This band defines a carbon–nitrogen bond order intermediate between a single bond (1250–1350 cm^{-1}) and a double bond (1640–1690 cm^{-1}) [51].

In the dithiocarbamate ligands, the bands in the region of 1457-1487 cm^{-1} are assigned to the ν(N-CSS) stretching vibrations. After complexation, these stretching bands are shifted to 1460-1501 cm^{-1}. Thus, showing an increase in the C-N double bond character [52]. This shift is caused by electron delocalization towards the metal ion upon coordination and confirmed the coordination of the metal ions to the dithiocarbamate ligands. As these frequency modes lie in between C-N and C=N bonds, the partial double bond character of the thioureido group was confirmed in complexes **1-5** [53].

The bands due to the –CSS moiety are usually coupled to other vibrations and are very sensitive to the environment of this group, which allows us to distinguish between monodentate and bidentate dithiocarbamate coordination. The presence of only one band in the region (940–1060) cm^{-1} was assumed by Bonati and Ugo [54] to indicate a completely symmetrical bonding of the dithiocarbamate ligand, which acts in a bidentate mode. On the other hand, a split band indicates a monodentate bound ligand. In this report, the presence of two bands in the investigated region, which is commonly attributed to monodentate coordination, suggests a monodentate asymmetrical behavior of the dithiocarbamate.

The coordination of phosphine and dithiocarbamate ligands with the Au(I) center *via* phosphorus and sulfur donor atoms is confirmed by the presence of *v*(Au-P) and *v*(Au-S) bands in the range of 272-289 and 195-202 cm^{-1} respectively in far-FTIR spectra. These observations agree with analogous data reported by other authors for similar compounds [55-57].

3.3. Solution NMR characterization

All ^{1}H NMR data supports the structures of synthesized complexes as indicated by the integration of signals of C-H protons of phosphine and dithiocarbamate groups. The ^{1}H NMR spectrum of complex **1** displays a doublet and singlet at 1.61 and 3.47 ppm corresponding to the methyl protons (9:6) of trimethylphosphine and dimethyldithiocarbamate ligands respectively (Figure 1S). Its ^{13}C NMR spectrum also confirms the structure of complex 1 as shown in Figure 2S. A complete list of ^{1}H and ^{13}C NMR data of complexes **(1-5)** along with their corresponding ligands and metal precursor is given in Tables 5S and 6S respectively. ^{1}H and ^{13}C NMR signals of alkyl groups of tertiary phosphine moiety are very close in the complexes (**1-5)**. There is no significant change in the $^{2}J_{P-H}$ coupling constant for the gold(I) precursor and their corresponding phosphanegold(I) dithiocarbamate complexes. The ^{31}P NMR spectra of the complexes (**1-5**) showed singlet

resonances and 1.6 to 2.8 ppm higher field shift compare to phosphine gold(I) chloride precursors was observed (Table 7S).

3.4. Solid-state NMR

At the spinning rate of 4 kHz, the isotropic signals for all complexes were observed for the carbon atom in NCS_2 fragment of the dithiocarbamate ligand, indicating the anisotropy that could take place due to the sp^2 hybridization of these atoms. Solid state NMR spectrum of free dialkyl dithiocarbamate ligands, chloridotriaethyl(phosphine)gold(I) and complexes **1-4** are shown in Table 8S. Complexes **1-4** showed significant downfield shifts (~ 4 ppm) that were observed for all carbons bonding to sulfur and phosphorus atoms in the dithiocarbamate and phosphine ligands, respectively, with respect to the free ligands. This can be attributed to the strong electron donation anticipated by S atom of the dimethyldithiocarbamate and P atom of trimethylphosphine. Compared to solution chemical shifts, significant de-shielding in solid state is observed with similarity in the chemical shift among all synthesized complexes which is a clear indication of stability of the prepared complexes in solid state.

3.5. Computational Study and Crystal structure of compound 1.

A single crystal X-ray molecular structure of $[Au(PMe_3)(S_2CNMe_3)]$ (**1**) is shown in Figure 1. In this structure gold(I) is coordinated with P and S donor atoms of trimethylphosphine and dimethyldithiocarbamate ligands respectively. The Au–S and Au–P bond distances are 2.326 (3) and 2.249 (3) Å respectively. The Au–P and Au–S bond distances are comparable with $[Au(PEt_3)(S_2CNEt_2)]$ complex [58]. The geometry around Au(I) metal atom is linear and S–Au–P bond angle is around 177° like other Au(I) complexes [59-62]. No significant intermolecular interactions have been observed in complex **1**. Only some non-standard H-bonds are present.

The optimized structure of the compound **1** as obtained from the B3LYP/LANL2DZ level of calculations are shown in Figure 2. There is a good agreement between the experimental and calculated structural parameters for almost all bond distances and angles, which provides more support to the crystallographic findings as given in Table 2.

3.6. *In vitro* cytotoxicity of gold(I) complexes against A549 and HepG2 cancer cell lines

The *in vitro* cytotoxic effect of gold(I) complexes **1-5** against two human carcinoma cell lines, A549 and HepG2, were studied using the MTT assay. The *in vitro* cytotoxic activity depends on the exposure time and the concentrations of the complexes. For that reason, we used different concentrations and a 3-day exposure protocol to determine the IC_{50} values for all five complexes along with cisplatin. The *in vitro* cytotoxicity in terms of IC_{50} values of cisplatin for both cell lines was included for comparison.

The IC_{50} data for the Au(I) complexes **1-5** showed *in vitro* cytotoxicity in a range of 4.87–7.06 μM, 5.76-8.35 μM for A549 and HepG2 cells, respectively. as given in Table 9S. For A549 cancer cell, the order of *in vitro* cytotoxicity in terms of IC_{50} values is complex **2** (4.87 μM) > complex **3** (6.58 μM), complex **4** (6.64 μM) > complex **1** (6.79μM) > complex **5** (7.06 μM) > cisplatin (29.76 μM). All the complexes showed significant cytotoxic effects and were found to be more active than cisplatin, specifically to be 4- to 6-fold more cytotoxic than cisplatin and to overcome both intrinsic and acquired resistance to cisplatin. Complex **2** is a reasonably better cytotoxic agent than are complexes **1, 3, 4** and **5**. For HepG2 cancer cell, the order of *in vitro* cytotoxicity in terms of IC_{50} values is complex **1** (5.76 μM) > complex **5** (6.21 μM) > complex **3** (6.90 μM) > complex **2** (7.41 μM) > complex **4** (8.35 μM) > cisplatin (30.53 μM). The complexes **1-5** showed significant cytotoxic effects better than cisplatin, specifically to be 3- to 5-folds more than cisplatin. Complex **1** is a reasonably better cytotoxic agent than complexes **2, 3, 4** and **5**.

In general, the anticancer activity of the synthesized complexes (**1-5**) against the A549 and HepG2 human cancer cell lines is interesting and exhibits better activity than in previous anticancer studies of gold compounds [63-66]. There is no doubt that this study is helpful for further exploiting and defining the potential role of dithiocarbamato(phosphine)gold(I) complexes in combat against lung and liver cancer.

3.7. DNA binding studies

Gold(I) complexes, beginning with auranofin, are gaining attention as a new class of chemotherapeutics because of their strong tumor cell growth-inhibiting effect [67]. Because DNA is the potential intracellular target for many anticancer drugs due to its predominant role in controlling cellular functions, the metallodrug–DNA interaction is very significant in view of its ability to function as a rational design system for the development of new efficient drugs that target DNA. DNA interaction can be achieved through intercalation between the metal complex and DNA, which results in hypochromism with or without a red/blue shift [68], and/or through non–intercalative/electrostatic interaction, which causes hypochromism [69].

3.8.1. Absorption spectral titrations

To evaluate the mode of interaction of complexes with CT–DNA, absorption titration studies have been performed by monitoring the changes in absorption intensity by aliquot addition of DNA. On addition of increasing concentrations (0–1.2 x 10^{-4} M) of CT DNA to a fixed amount (0.67 x 10^{-4} M) of complexes **1–5** there was change in absorption intensity in ligand–based $\pi\rightarrow\pi^*$ transitions centerd at ca. 270 nm exhibiting significant "hyperchromism" (43–20%) along with blue shift of 5–2 nm (Figure 5a–e). The resultant hyperchromic shift suggests that all the complexes bind to CT–DNA by the external contact, possibly due to electrostatic binding [70]. The intrinsic binding constant, K_b is a useful tool to monitor the magnitude of the binding strength of complexes with CT–DNA (Table 10S). K_b values followed the order **4** > **3** > **2** > **1** > **5**, indicating that the complex **4**

bind more avidly to CT-DNA in comparison to other analogous. The relative difference in the K_b values could be attributed to different binding modes of Au(I) complexes depending upon the type of substituent groups. Since, lipophilicity and hydrophilicity of the gold complexes is a very important parameter in optimizing biodistribution, activity and selectivity of the drugs thus the nature of the ligands attached to the gold atom is a valuable parameter for drug design. Previous structure-activity relationship studies on linear, gold(I) complexes indicated that the presence of the phosphine ligand is important for the biological potency of the complexes [71]. Long alkylic chains lead to more hydrophobicity and consequently accounting for higher binding affinity with DNA as compared to their short–chained analogs. This could be the reason for higher binding affinity of complex **4**, however, in case of **5** the bulkier isopropyl moiety of phosphine could induce steric constraints resulting in the lower binding propensity with DNA.

3.8.2. Interaction with nucleotides

To obtain concrete information and to determine the coordination of the metal ion to the specific site at the molecular target, interactions with low molecular building blocks of large DNA molecules *viz.,* 5'–GMP, 5'–TMP, 5'–AMP and 5'–CMP were carried out with the complex **4**. The intrinsic binding constant (K_b) values of complexes (**1-5**) with CT DNA are given in Table 10S. On addition of increasing amounts of mononucleotides to the complex **4**, hypochromic effect was observed with concomitant moderate blue shift (2–5 nm) at $\pi \rightarrow \pi^*$ (Figure 6a–d), implicating the electrostatic surface binding interactions of **4** with different nucleotides. The purine and pyrimidine bases of CT–DNA become exposed because of the unwinding of the DNA duplex promoting an effective binding to these base pairs with the drug entities. To compare quantitatively the binding extent of complex **4** towards mononucleotides (5'–GMP, 5'–TMP, 5'–AMP and 5'–CMP), the intrinsic binding constants (K_b) were determined and found to be 3.3×10^4, 4.9×10^4, 5.7×10^4 and 2.8×10^4 M^{-1}, respectively. The trend of mononucleotide interaction with **4,** as validated by K_b values was 5'–AMP > 5'–TMP >

5'–GMP > 5'–CMP, supports the preferential selectivity for guanine residue by the coordination with N7 atom of the (guanine) base of DNA duplex.

3.8.3. Fluorescence spectral studies

The fluorescence emission titration of complexes **1–5** were carried out in order to have deep insight into the nature of binding mode of these complexes with CT–DNA because of its high sensitivity, good repeatability and accuracy. In the absence of CT–DNA, all complexes **1–5** emit strong luminescence when excited at 275 nm in Tris–HCl/NaCl buffer with an emission maximum appearing at 340 nm. However, the subsequent addition of CT–DNA from 0.067–0.33 x 10^{-4} M causes a gradual enhancement in the fluorescence intensity of the complexes with no apparent change in the shape and position of the emission bands (Figure **7**a–e) indicative of strong interaction of the Au(I) drug entities with CT DNA. The hydrophobic molecular structure of CT DNA could be responsible for enhancing the fluorescence quantum yield of complexes, leading to the higher fluorescence intensity with increasing concentration of CT DNA. In addition, energy transfer from CT–DNA to metal complexes could also induce fluorescence enhancement [72, 73]. The Scatchard binding constant, K values of **1–5** were found to be 2.8 x 10^4, 3.5 x 10^4, 5.7 x 10^4, 6.6 x 10^4 and 1.9 x 10^4 M^{-1}, respectively with mean standard deviations of ±0.07. These results are consistent with the findings obtained from UV–vis spectral studies.

3.8.4. Ethidium bromide displacement assay

A reliable method for studying the binding of molecules to nucleic acids is the fluorescence quenching method. Ethidium bromide (EB) is a planar cationic dye which is widely used as a sensitive fluorescence probe for native DNA. EB emits intense fluorescent light in the presence of DNA due to its strong intercalation between the adjacent DNA base pairs. The displacement technique is based on the decrease of fluorescence resulting from the displacement of EB from a

DNA sequence by a quencher, and the quenching is due to the reduction of the number of binding sites on the DNA that are available to the EB [74]. The emission spectra of DNA–EB system in the absence or presence of **1–5** are shown in Figure 8a–e. Upon increasing concentrations of complexes **1–5**, the fluorescence intensity of CT-DNA previously treated with EB at 585–590 nm showed a remarkable decreasing trend, suggesting that the Au(I) analogs bind significantly to DNA. Furthermore, the quenching extents were quantitatively evaluated by employing Stern–Volmer equation and K_{SV} values for **1–5** were found to be 0.19, 0.34, 0.67, 0.91 and 0.10, respectively. From the above data it is clear that **4** replaces EB more effectively relative to other complexes which is in agreement with the results obtained from electronic absorption studies.

4. Molecular docking studies

Au(I) drug entities **1–5** were successively docked with the DNA duplex of the sequence d(CGCGAATTCGCG)$_2$ dodecamer (PDB ID: 1BNA) in order to predict the chosen binding site along with preferred orientation inside the DNA minor groove. The study revealed that complexes under investigation interact with DNA *via* an electrostatic mode involving outside edge stacking interaction with oxygen atom of the phosphate backbone. From the energetically most favorable conformation of the docked poses (Figure 12a–e) it is clear that Au(I) analogous **1–5** fit well into the minor groove of the targeted DNA and stabilized the A−T rich region by van der Waals interactions with the DNA functional groups that define the stability of the groove [75]. It believes that dithiocarbamate ligand containing sulphur donor atoms offers stabilization to produce viable interaction with the DNA. Relative binding energy of the docked structures was found to be −166.41, **1**; −172.82, **2**; −180.75, **3**; −188.27, **4**; and −161.27 kJ mol^{-1}, **5**. These are consistent with the spectral studies and clearly implicated that complex **4** has greater DNA binding affinity relative to other complexes. Thus, results suggested that there is good correlation between spectroscopic results and molecular modeling.

Conclusion

In current study, the cytotoxic activity of five gold(I) complexes against A549 and HepG2 human cancer cell lines was evaluated. All complexes (**1-5**) showed excellent cytotoxic activity against both cell lines (A549, HepG2). The IC_{50} data reveals that complexes **1-5** are better cytotoxic agent than cisplatin a commercial drug. Structural changes may substantially alter the DNA binding mode and DNA damage; thus a comparative *in vitro* interaction study was conducted with CT DNA. Molecular docking studies revealed that the synthesized gold(I) complexes (**1-5**) can induce the distortion of DNA double helix. This observation suggests that gold(I) complexes are targeting intracellular DNA *in vitro.* Enhanced and better *in vitro* cytotoxicity of this class of gold(I) complexes than a commercial chemotherapeutic drug merits them for further *in vivo* investigations as anticancer agents.

Supplementary material

Supplementary crystallographic data of CCDC deposit number is 1006138 for the complex **1** and can be obtained free of charge via www.ccdc.cam.ac.uk/data_request/cif, by e-mailing data_request@ccdc.cam.ac.uk, or by contacting the Cambridge Crystallographic Data Centre, 12 Union Road, Cambridge CB2 1EZ, UK; fax: +44(0)1223-336033.

Acknowledgement

This project was funded by the National Plan for Science and Innovation (MARIFAH)–King Abdulaziz City for Science and Technology (KACST) through the Science and Technology Unit at King Fahd University of Petroleum and Minerals (KFUPM) of Saudi Arabia, award No. **14-MED64-04**. The authors greatly appreciate and thank the financial support provided by King Fahd University of Petroleum and Minerals under the project No. **IN151022.** The authors also thankful to the Deanship of Scientific Research and College of Pharmacy Research Center, King Saud University for their support.

References

[1] R.W. Sun, M. Zhang, D. Li, Z. Zhang, H. Cai, M. Li, Y. Xian, S. W. Ng, A.S. Wong, J. Chem. Eur. 21 (2015) 18534–18538.

[2] M. Altaf, S. Ahmad, A. Kawde, N. Baig, A. Alawad, S. Altuwaijri and Helen Stoeckli-Evans and A. A. Isab**,** New J. Chem., 40 (2016) 8288-8295.

[3] L.S. Best, J.P. Sadler, Gold Bull. 29 (1996) 87–93.

[4] M.J. Chow, C. Licona, G. Pastorin, G. Mellitzer, W.H. Ang, C. Gaiddon, Chem. Sci. 7 (2016) 4117-4124.

[5] N. Pantelic, T.P. Stanojkovic, B.B. Zmejkovski, T.J. Sabo, G.N. Kaluderovic, Eur. J. Med. Chem. 90 (2015) 766–774.

[6] S.S. Al-Jaroudi, M. Fettouhi, M.I.M. Wazeer, A.A. Isab, S. Altuwaijri. Polyhedron 50 (2013) 434−442.

[7] B. Bertrand, E. Bodio, M. Richard Picquet, P. Le Gendre, A. Casini, 775 (2015) 124–129.

[8] B. Rosenberg, L. Van Camp, T. Krigas, Nature 205 (1969) 698- 699.

[9] G. Xu, J. Lin, W. Li, J. Zhao, S. Gou, Inorg. Chim. Acta. 462 (2017) 188–194.

[10] P. Lee, R. Zhang, V. Li, X. Liu, R.W.Y. Sun, C-M. Che, K.K.Y. Wong, Int. J. Nanomed. 7 (2012) 731−737.

[11] G. Adams, J. Zekri, H. Wong, J. Walking, J.A. Green, BJOG 117 (2010) 459−1467.

[12] T.R.E. Tiekink, Inflammopharmacology 16 (2008)138–142.

[13] I. Ott, Coord. Chem. Rev. 253 (2009) 1670–1681.

[14] A. Pratesi, D. Cirri, M. Đurović, S. Pillozzi, G. Petroni, Ž.D. Bugarčić, L. Messori, Biometals. 29 (2016) 905–911.

[15] W. Walther, O.Dala, C. O'Beirne, I. Ott, G. Sánchez-Sanz, C. Werner, X. Zhu, M. Tacke, Lett. Drug. Design. Discov. 14 (2017) 125–134.

[16] M. Altaf, M. Monim-ul-Mehboob, M. Ogasawara, N. Casagrande, M. Celegato, C. Borghese, Z.H. Siddik, D. Aldinucci, A.A. Isab, Oncotarget, 8 (2017) 490-505.

[17] D. Fregona, L. Giovagnini, L. Ronconi, C. Marzano, A. Trevisan, S. Sitran, B. Biondi, F. Bordin, J. Inorg. Biochem. 93 (2003) 181−189.

[18] D. de Vos, S.Y. Ho, E.R.T. Tiekink, Bioinorg. Chem. Appl. 2 (2004) 141–145.

[19] V. Gandin, A.P. Frenandes, M.P. Rigobello, B. Dani, F. Sorrntino, M. Björnstedt, A. Bindoli, A. Sturaro, R. Rella, C. Marczano, Biochem. Pharma. 79 (2010) 90–101.

[20] B-J. Chen, N.S. Jamaludin, C-H. Khoo, T-H. See, J-H. Sim, Y-K. Cheah, S.N. Abdul Halim, H-L. Seng, E.R.T. Tiekink, J. Inorg. Biochem. 163 (2016) 68–80.

[21] E.M. Kinsch, D.W. Stephan, Inorg. Chim. Acta 91 (1984) 263-267.

[22] V. Gandin, K. Fritz-Wolf, R. Reau, C. Herold-Mende, K. Toth, E. Davioud-Charvet, K. Becker, Angew. Chem. Int. Ed. 45 (2006) 1881–1886.

[23] R.F. Keene, A.J. Smith, G.J. Collins, Coord. Chem. Rev. 253 (2009) 2021–2035.

[24] M. Sirajuddin, S. Ali, A. Badshah, J. Photochem. Photobiol. B 124 (2013) 1–19.

[25] M. Altaf, M. Monim-ul-Mehboob, A.A. Seliman, M. Sohail, M.I.M. Wazeer, A.A. Isab, L. Li, V. Dhuna, G. Bhatia, K. Dhuna, Eur. J. Med. Chem. 95 (2015a) 464–472.

[26] M. Altaf, M. Monim-ul-Mehboob, A.A. Isab, G. Bhatia, K. Dhuna, S. Altuwaijri, New J. Chem. 39 (2015) 377–385.

[27] K. Al-Sa'ady, A. McAuliffe, V.R. Parish, A.J.A. Sandbank, Inorg. Synth. 23 (1985) 191–194.

[28] Stoe, Cie (2006) X-Area V1.35 and X-RED32 V1.31 Software, Stoe and Cie GmbH, Darmstadt Germany.

[29] M.G. Sheldrick, Acta Cryst. A64 (2008) 112–122.

[30] L.A. Spek, Acta Cryst. D65 (2006) 148–155.

[31] F.C. Macrae, R.P. Edgington, P. McCabe, E. Pidcock, P.G. Shields, R. Taylor, M. Towler, J. Van de Streek, J. Appl. Cryst. 39 (2006) 453–457.

[32] J.M. Frisch, W.G. Trucks, B.H. Schlegel, E. G. Scuseria, A.M. Robb, J.R. Cheeseman, G. Scalmani, V. Barone, B. Mennucci, A.G. Petersson, H. Nakatsuji, M. Caricato, X. Li, P.H. Hratchian, F.A. Izmaylov, J. Bloino, G. Zheng, L.J. Sonnenberg, M. Hada, M. Ehara, K.Toyota, R. Fukuda, J. Hasegawa, M. Ishida, T. Nakajima, Y. Honda, O. Kitao, H. Nakai, T. Vreven, A.J. Montgomery, E.J. Peralta, F. Jr Ogliaro, M. Bearpark, J. J. Heyd, E. Brothers E N. K. Kudin, N. V. Staroverov, R. Kobayashi, J. Normand, K. Raghavachari, A. Rendell, C. J. Burant, S. S. Iyengar, J. Tomasi, M. Cossi, N. Rega, M.J. Millam, M. Klene, E.J. Knox, B.J. Cross, V. Bakken, C. Adamo, J. Jaramillo, R. Gomperts, E.R. Stratmann, O. Yazyev, A.J. Austin, R. Cammi, C. Pomelli, W.J. Ochterski, L.R. Martin, K. Morokuma, G.V. Zakrzewski, A.G. Voth, P. Salvador, J.J. Dannenberg, S. Dapprich, D.S. Daniels, O. Farkas, B. J. Foresman, V.J. Ortiz, J. Cioslowski, J.D. Fox, Gaussian 09 Revision A1 Gaussian Inc. Wallingford CT (2009).

[33] D.A. Becke, Phys. Rev. 38 (1988) 3098–3100.

[34] C.W. Lee, W. D. Yan, G. R. Parr, Deve. Phys. Rev. B 37 (1988) 785–789.

[35] J.P. Hay, R.W. Wadt, J. Chem. Phys. 82 (1985a) 270–282.

[36] R. W. Wadt, J. P. Hay, J. Chem. Phys. 82 (1985) 284–298.

[37] J. P. Hay, R. W. Wadt, J. Chem. Phys. 82 (1985b) 299–310.

[38] J. Marmur, J. Mol. Biol. 3 (1961) 208–218.
[39] J.P. Naskar, B. Guhathakurta, P. Basu, N. Bandyopadhyay, G.S. Kumar, M. Zhu, L. Lu, Inorg. Chim. Acta. 462 (2017) 158–166.
[40] M. Chauhan, K. Banerjee, F. Arjmand, Inorg. Chem. 46 (2007) 3072–3082.
[41] A. Wolfe, H.G. Shimer, T. Meehan, Biochem. 26 (1987) 6392–6396.
[42] D.G. Liu, P.J. Liao, Z.Y. Fang, S.S. Huang, L.G. Sheng, Q.R. Yu, Anal. Sci. 18 (2002) 391–395.
[43] F.E. Healy, J. Chem. Educ. 84 (2007) 1304–1307.
[44] R.J. Lakowiez, G. Webber, Biochem. 12 (1973) 4161– 4170.
[45] Y. Yang, B. Zuo, J.G. Li, G. Chen, Spectrochim. Acta Part A 52 (1996) 1915–1919.
[46] Q.Q. Liao, Y.Z. Wang, J.Y. Li, B. Xiang, M.R. Cheng, J.Q. Zhang, Spectrosc. Spectr. Anal. 29 (2009) 829–832.
[47] Y.Y. Jia, Y. B. Gao, L. Lu, N.X. Wang, M.X. Xu MX, China Environ. Sci. 29 (2009) 201–206.
[48] A.P. Ajibade, G.O. Idemudia, A. Okoh, Bull. Chem. Soc. Ethiop. 27 (2013) 77−84.
[49] N. Nakamoto, J. Fujita, R.A. Condrote, Y. Morimoto, J. Chem. Phys. 39 (1963) 423–427.
[50] G. Durgaprasad, N.D. Sathyanarayana, C.C. Patel, Can J. Chem. 47 (1969) 631–635.
[51] J.A. Odola, O.A.J. Woods, J. Chem. Pharm. Res. 3 (2011) 865–871.
[52] W.A. Herlimger, N.S. Wenhold, V.T. Long, J. Am. Chem. Soc. 92 (2007) 6474–6481.
[53] F. Jian, Z. Wang, Z. Bai, X. You, H. Fun, K. Chinnakali, A.L. Razak, Polyhedron 18 (1999) 3401–3406.
[54] F. Bonati, R. Ugo, J. Organomet. Chem. 10 (1967) 257–268.
[55] N.K. Kouroulis, K.S. Hadjikakou, N. Kourkoumelis, M. Kubicki, L. Male L, M. Hursthouse, S. Skoulika, K.A. Metsios, Y.V. Tyurin, V.A. Dolganov, R.E. Milaevag, N. Hadjiliadis, Dalton Trans. (2009) 10446–10456.
[56] A.E. Allen, W. Wilkinson. Spectrochim Acta 2 (1972) 2257–2262.
[57] G. A. Jones, B.D. Powell, Spectrochim. Acta 30 (1974) 563–570.
[58] Y.S. Ho, T.R.E. Tiekink, Z Kristallogr NCS 220 (2005) 342–344.
[59] I. Sänger, W.H. Lerner, T. Sinke, M. Bolte, Acta Cryst. (2012) E68 m708.
[60] P. Lu, C.T. Boorman, Z.M.A. Slawin, I. Larrosa, J. Am. Chem. Soc. 132 (2010) 5580–5581.
[61] E.R. Marsh, Acta Cryst. B 58 9 (2002) 893–899.
[62] H. Schmidbaur, B. Brachthiuser, O. Steigelmann, H. Beruda, Chem. Ber. 125 (1992) 2705–2710.

[63] E. Barreiro, S.J. Casas, D.M. Couce, A. Sánchez, J. Sordo, M.E. Vázquez-López, J Inorg Biochem. 131 (2014) 68–75.

[64] R. Kivekäs, E. Colacio, J. Ruiz, D.J. López-González, P. León, Inorg. Chim. Acta 159 (1989) 103–110.

[65] L. Ortego, F. Cardoso, S. Martins, F.M. Fillat, A.M. Laguna, M. Meireles, D.M. Villacampa, C.M. Gimeno, J. Inorg. Biochem. 130 (2014) 32–37.

[66] I. Ott, T. Koch, H. Shorafa, Z. Bai, D. Poeckel, D. Steinhilber, R. Gust, Org. Biomol. Chem. 3 (2005) 2282–2286

[67] S. Nobili, E. Mini, I. Landini, C. Gabbiani, A. Casini, L. Messori, Med. Chem. Res. 30 (2010) 550−580.

[68] Z.C. Liu, B.D. Wang, B. Li, Q. Wang, Z.Y. Yang, T.R. Li, Y. Li, Eur. J. Med. Chem. 45 (2010) 5353–5361.

[69] L. Tjioe, A. Meininger, T. Joshi, L. Spiccia, B. Graham, Inorg. Chem. 50 (2011) 4327–4339.

[70] G. Kalaiarasi, R. Jain, A. Shanmugapriya, H. Puschman, P. Kalaivani, R. Prabhakaran, Inorg. Chim. Acta. 462 (2017) 174–187.

[71] T. Zou, C.T. Lum, C-N. Lok, J-J. Zhang, C-M. Che, Chem. Soc. Rev. 44 (2015) 8786-8801.

[72] F. Arjmand, A. Jamsheera, M.S. Afzal, S. Tabassum, Chirality 24 (2012) 977–986.

[73] S. Tabassum, S. Yadav, F. Arjmand, J. Organomet. Chem. 745–746 (2013) 226–234.

[74] E. Ramachandran, S.D. Raja, P.S. Bhuvanesh, K. Natarajan, Dalton Trans. 41 (2012) 13308–13323.

[75] T.J. Wang, Q. Xia, H.X. Zheng, Y.H. Chen, H. Chao, W.Z. Mao, N.L. Ji, Dalton Trans. 39 (2010) 2128–2136.

581

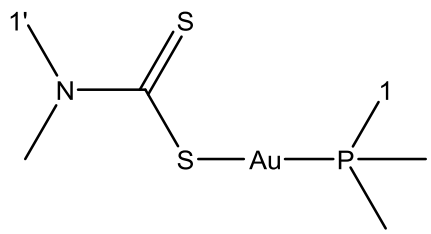

[(DMDT)Au(I)(P{Me}$_3$)] **(1)**

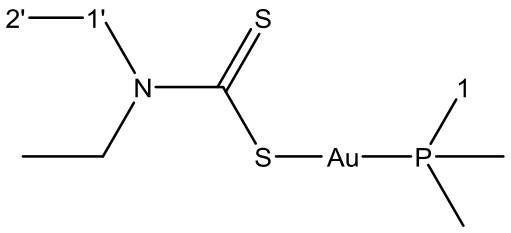

[(DEDT)Au(I)(P{Me}$_3$)] **(2)**

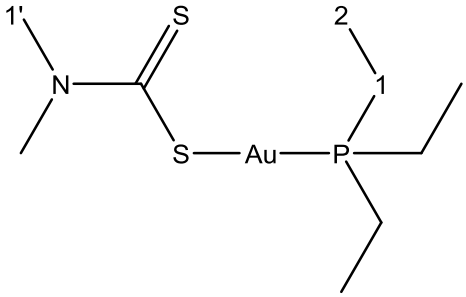

[(DMDT)Au(I)(P{Et}$_3$)] **(3)**

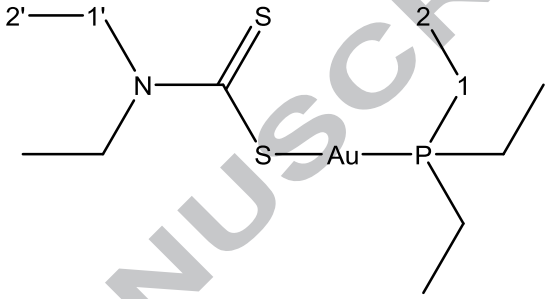

[(DEDT)Au(I)(P{Et}$_3$)] **(4)**

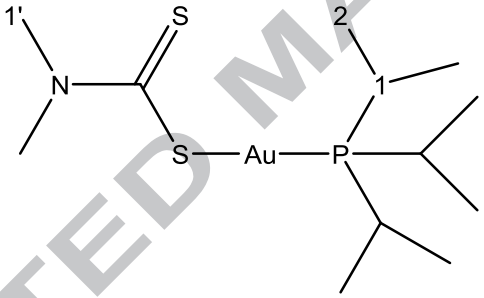

[(DMDT)Au(I)(P{i-Pr}$_3$)] **(5)**

582

583

584 **Scheme 1**. Chemical structure of the synthesized **1-5** complexes

585

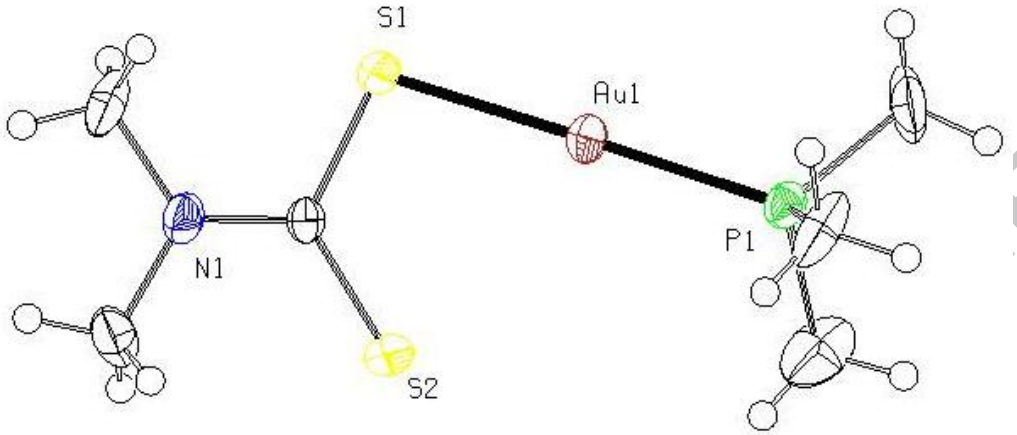

Figure 1. A view of the molecular structure of mononuclear complex **1**, with partial atom labelling scheme and displacement ellipsoids drawn at 50% probability level.

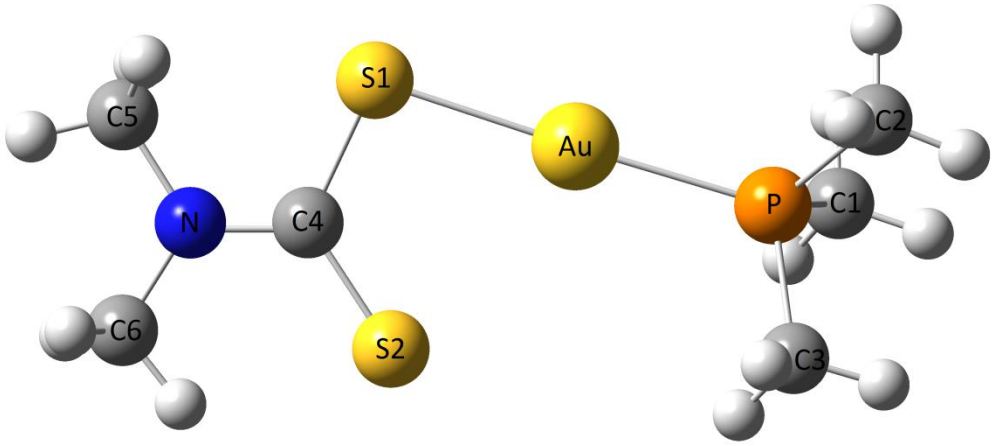

Figure 2. Optimized geometry of complex **1**, obtained at the B3LYP/LanL2DZ level of theory using GAUSSIAN09 W.

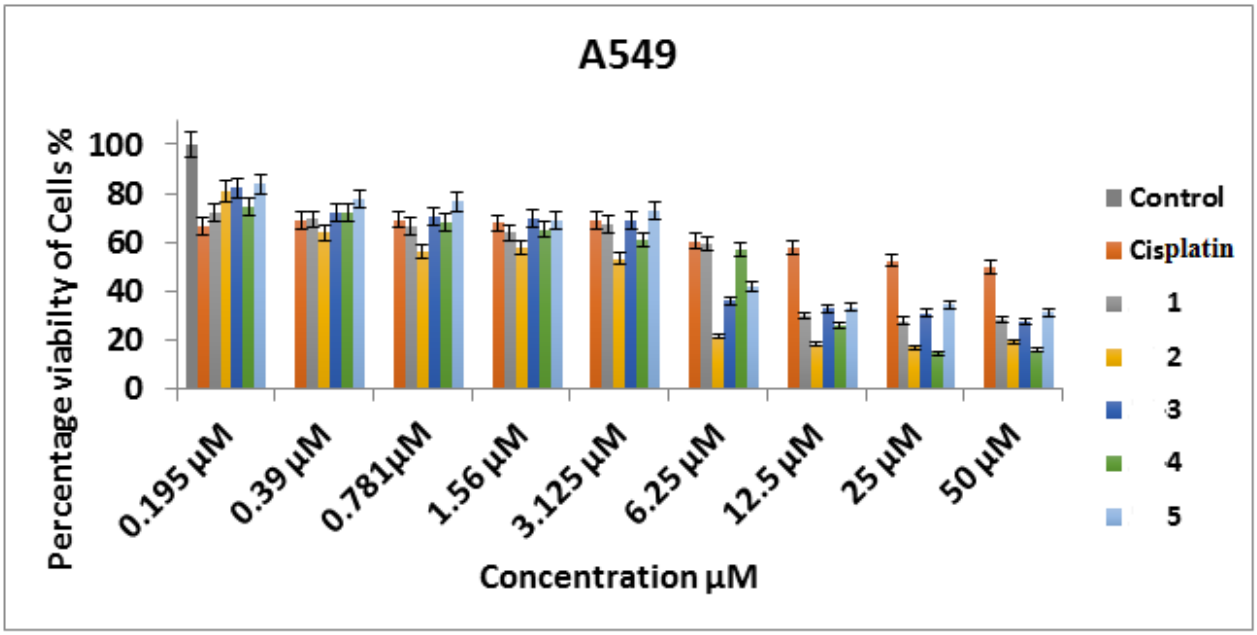

Figure 3. Cytotoxic effect of series of concentrations of compounds (**1-5**) on viability of A549 cells.

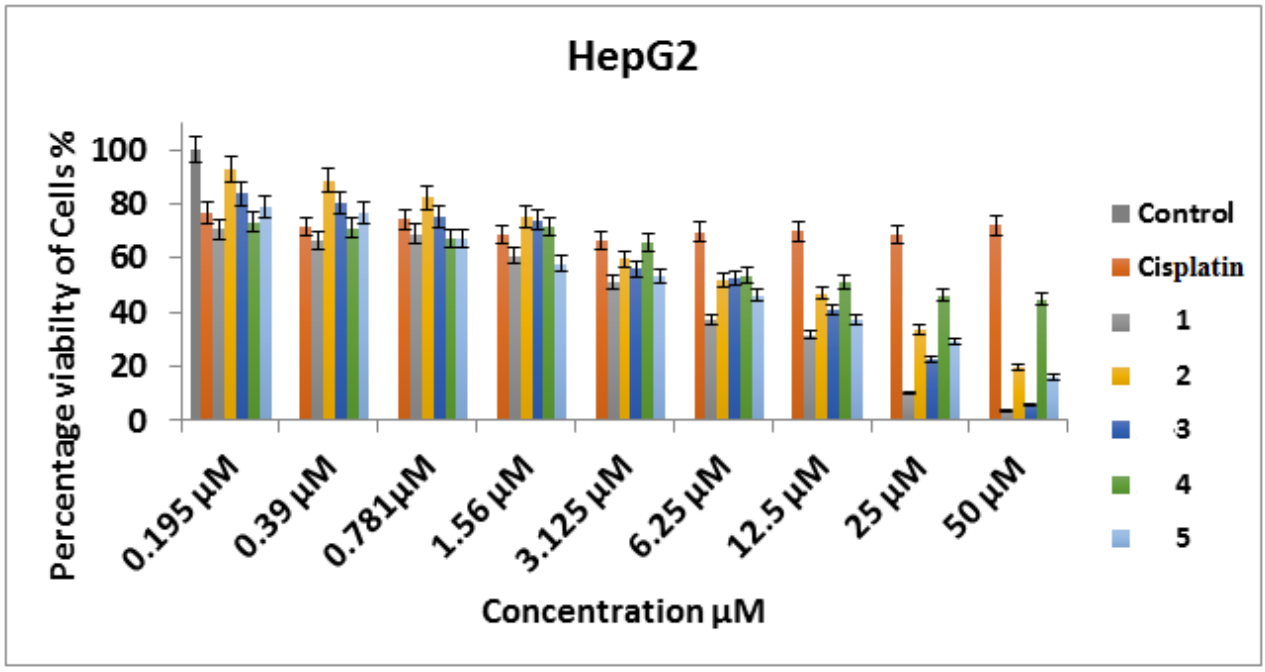

Figure 4. Cytotoxic effect of series of concentrations of compounds (**1-5**) on viability of HepG2 cells.

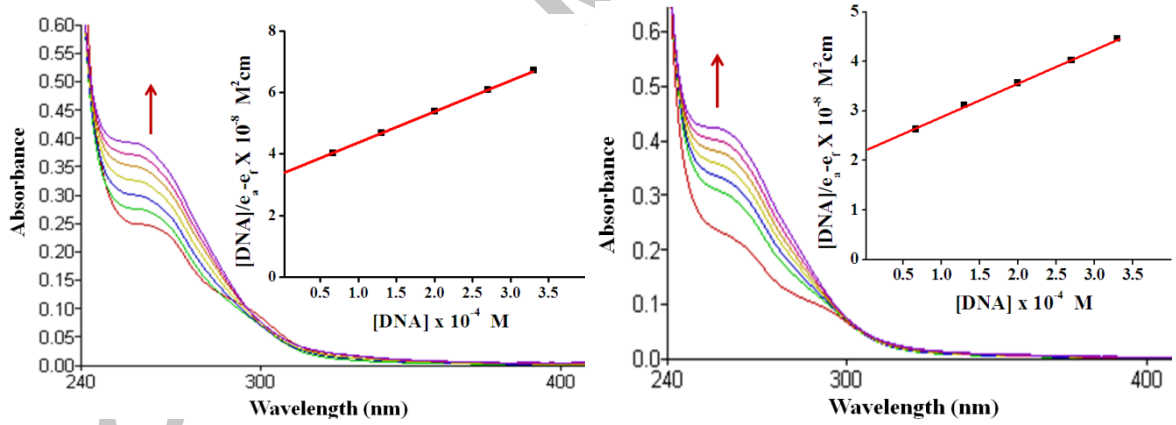

(a) **(b)**

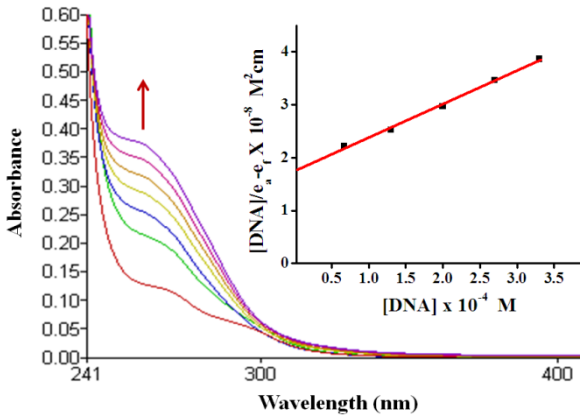

(c)

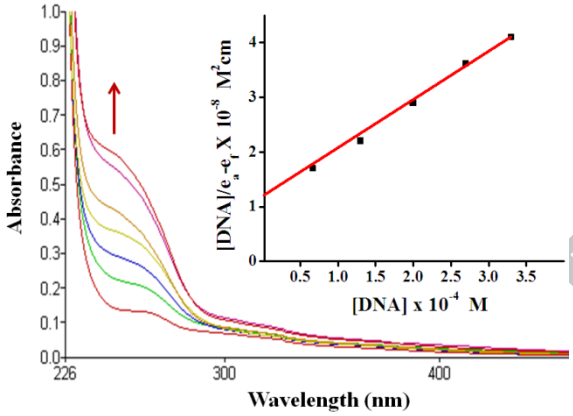

(d)

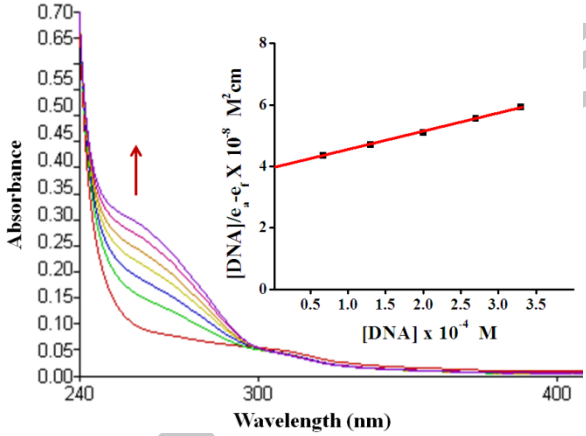

(e)

Figure 5. Absorption spectra of complex (a) **1**, (b) **2**, (c) **3**, (d) **4** and (e) **5** in the absence and presence of CT DNA. Inset: Plots of $[DNA]/(\varepsilon_a-\varepsilon_f)$ vs. [DNA] for the titration of CT DNA with complexes. [Complex] = 1.3 x 10^{-4} M, [CT DNA] = 0–1.2 x 10^{-4} M.

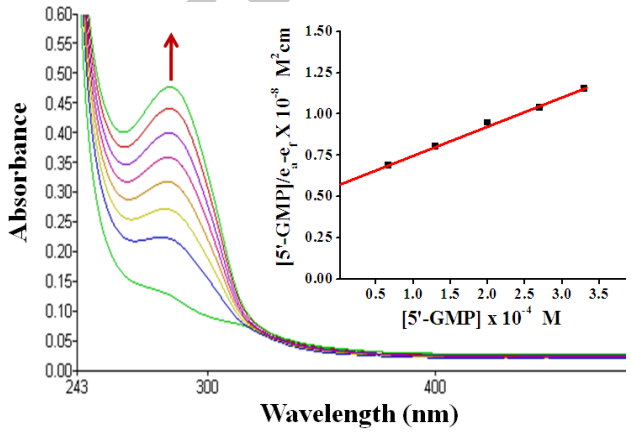

(a)

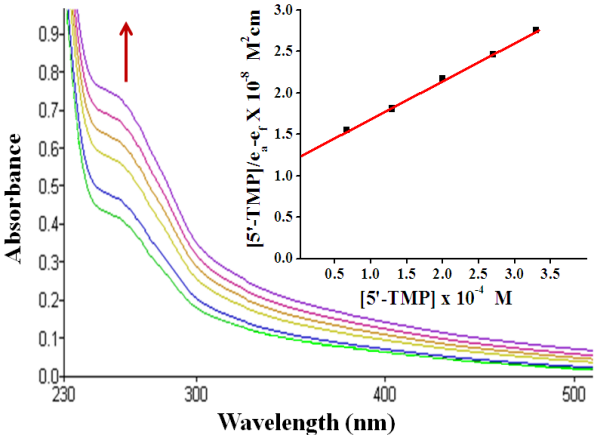

(b)

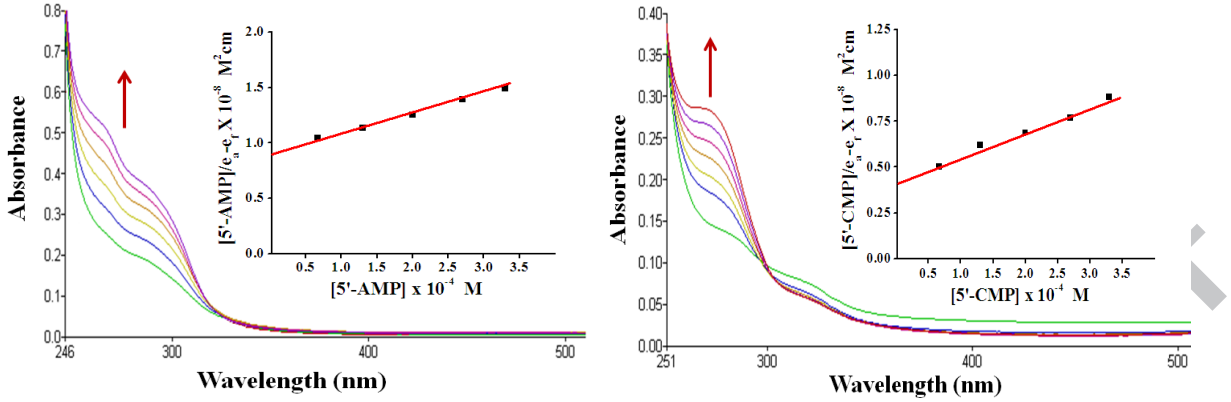

(c) **(d)**

Figure 6. Absorption spectra of **4** (1 x 10^{-4} M) in Tris–HCl buffer, on interacting with (a) 5'–GMP, (b) 5'–TMP, (c) 5'–AMP and (d) 5'–CMP at 10^{-4} M at 25 °C.

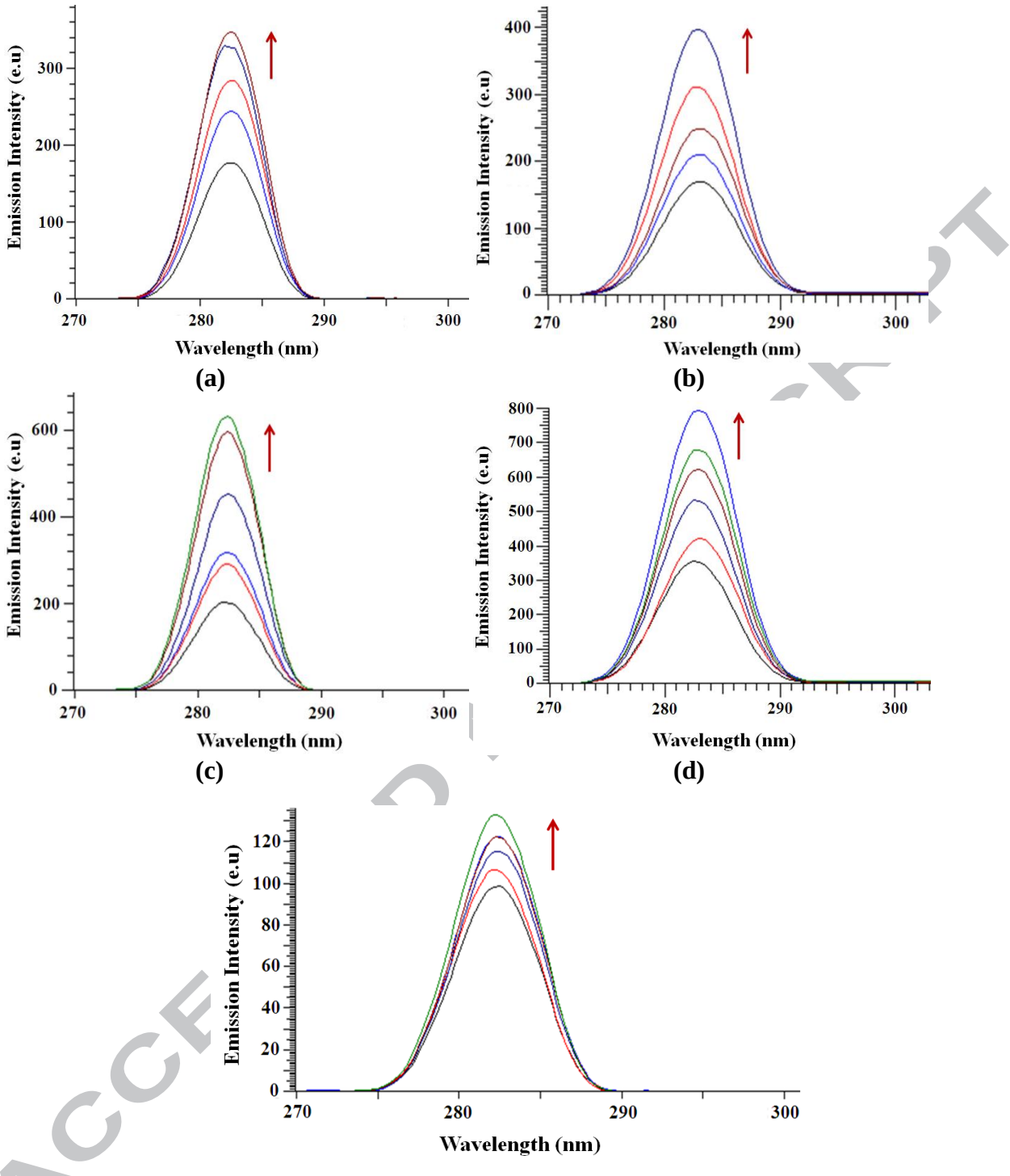

Figure 7. Emission spectra of complex (a) **1**, (b) **2**, (c) **3**, (d) **4** and (e) **5** in Tris–HCl buffer (pH = 7.2) in the absence and presence of CT DNA. [Complex] = 1.3 x 10^{-4} M, [DNA] = 0–0.50 x 10^{-4} M. Arrows indicate the change in emission intensity upon increasing the DNA concentration.

637

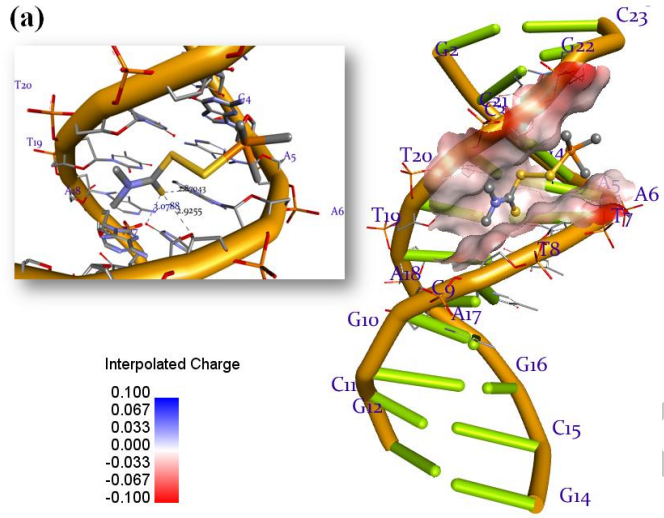

638

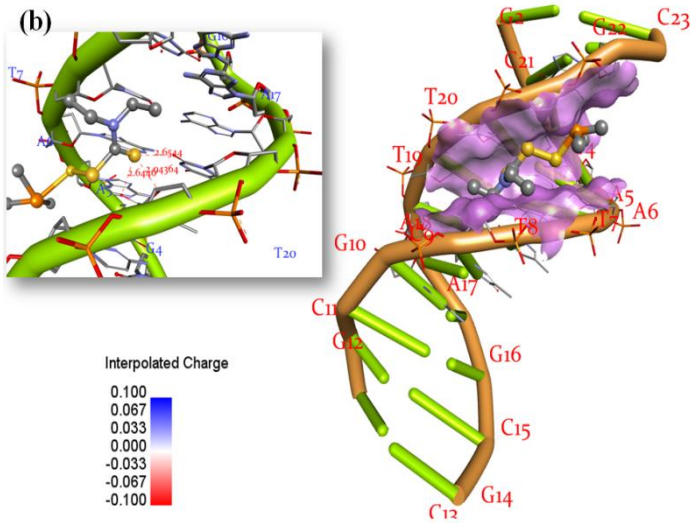

639

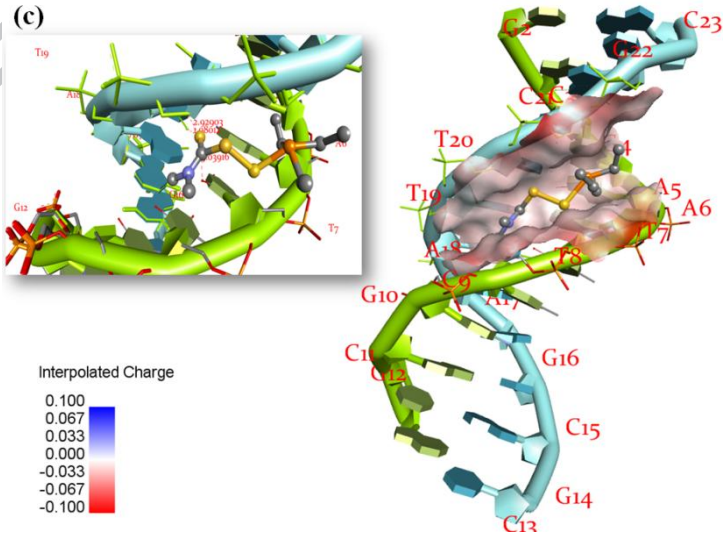

640

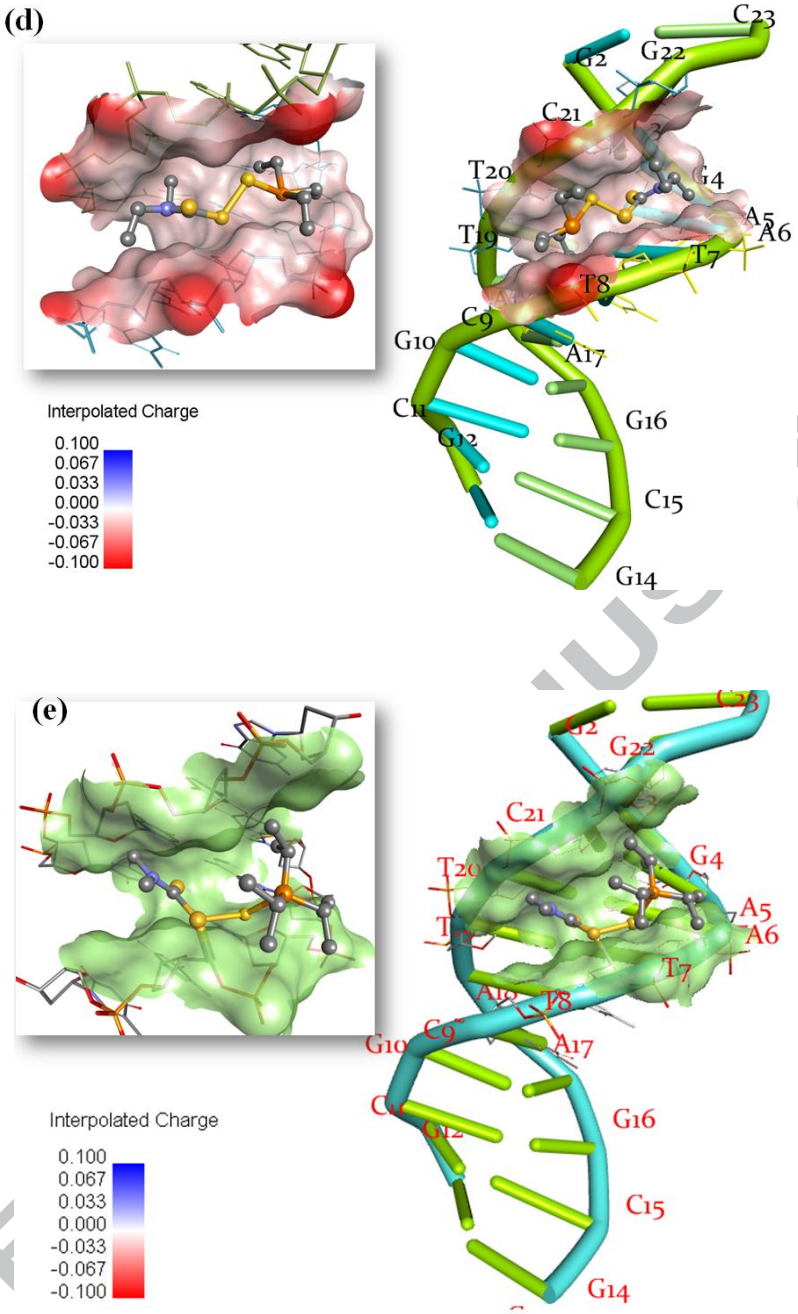

641

642

643

644

645 **Figure 8.** Molecular docked models of complex (a) **1**, (b) **2**, (c) **3**, (d) **5** and (e) **4** with DNA [dodecamer
646 duplex of sequence d(CGCGAATTCGCG)$_2$ (PDB ID: 1BNA)].

647

648

649 **Table 1**. Summary of crystal data and details of the structure refinement for complex **1.**

Complex	**1**
Emperical formula	$C_6H_{15}AuNPS_2$
Formula weight	393.25
Crystal size/mm	0.45 × 0.42 ×
Wavelength/Å	0.40
Temperature/K	0.71073
Crystal symmetry	173 (2)
Space group	Orthorhombic
a/Å	Fdd2
b/Å	32.075 (2)
c/Å	24.0898 (14)
V/ Å^3	6.1700 (3)
Z	4767.4 (5)
D_x (Mg m^{-3})	16
μ (mm^{-1})	2.192
F(000)	12.78
θ Limits/°	2944
No. of measured, independent an	2.1–25.7
observed $[I > 2\sigma(I)]$ reflections	8133, 2174, 2175
R_{int}	
Goodness of fit on F^2	0.179
$R[F^2 > 2\sigma(F^2)]$	1.07
$wR(F^2)$	0.046
$\Delta\rho_{max}$, $\Delta\rho_{min}$ (e Å^{-3})	0.118
T_{min}, T_{max}	1.63, −3.73
	0.286, 1.000

650
651
652
653
654
655
656
657
658
659

660

661

662 **Table 2.** Selected bond distances and bond angles for complex **1.**

Compound **1**			
Bond Length (Å), found [Calc.]		Bond Angles (°), found [Calc.]	
Au—P1	2.249 (3) [2.396]	P1—Au—S1	176.88 (13) [178.3]
Au—S1	2.326 (3) [2.453]	C1—P1—C2	103.7 (10) [104.0]
P1—C1	1.775 (16) [1.881]	C1—P1—C3	104.1 (9) [104.1]
P1—C2	1.792 (14) [1.881]	C2—P1—C3	105.0 (8) [104.2]
P1—C3	1.797 (15) [1.879]	C1—P1—Au	117.5 (6) [116.3]
S1—C4	1.758 (12) [1.826]	C2—P1—Au	113.1 (6) [112.3]

663

664

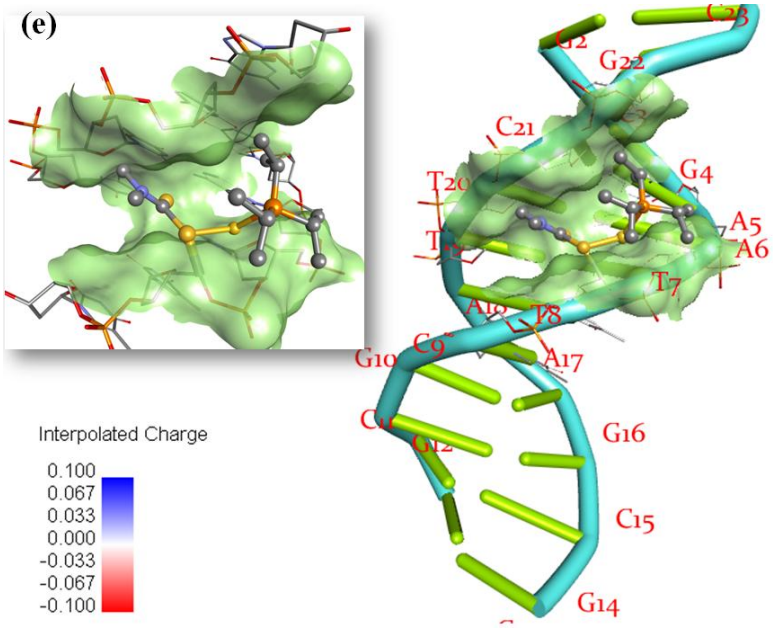

665

666

667

668

669 Molecular docked models of complex [(DEPT)Au(I)(P{Et_3}] with DNA [dodecamer duplex of

670 sequence d(CGCGAATTCGCG)$_2$ (PDB ID: 1BNA)].

671

672

- New dithiocarbamate phosphine Au(I) complexes were synthesized as antitumor chemotherapeutic agents.
- All complexes exhibited strong *in vitro* cytotoxic effects against A549 and HepG2 cell lines more than the well-known cisplatin.
- Molecular docking studies of the Au(I) complexes were conducted with B–DNA to visualize the preferential docking position.
- In $[(CH_3)_3PAu(S_2CN\{CH_3\}_2)]$ structure, the gold(I) is coordinated with one P donor atom of trimethylphosphine and S donor atom of dimethyldithiocarbamate ligand molecules.